Front. Environ. Sci. Eng. 2018, 12(1): 6
https://doi.org/10.1007/s11783-018-1022-2

RESEARCH ARTICLE

Significant enhancement in catalytic ozonation efficacy: From granular to super-fine powdered activated carbon

Tianyi Chen[1], Wancong Gu[1], Gen Li[2], Qiuying Wang[1], Peng Liang[1], Xiaoyuan Zhang (✉)[1], Xia Huang (✉)[1]

1 State Key Joint Laboratory of Environment Simulation and Pollution Control, School of Environment, Tsinghua University, Beijing 100084, China
2 Department of Urban Construction, Wuhan University of Science and Technology, Wuhan 400065, China

HIGHLIGHTS

- SPAC significantly enhanced the efficacy of catalytic ozonation.
- Large external surface reduced the diffusion resistance.
- Surface reaction was dominant for SPAC-based catalytic ozonation.
- Simple ball milling brought favorable material characteristics for catalysis.

GRAPHIC ABSTRACT

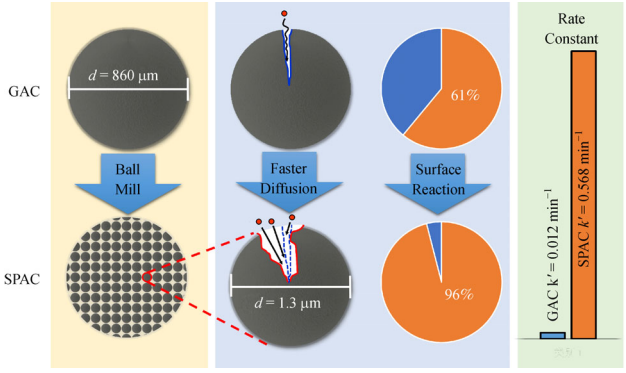

ARTICLE INFO

Article history:
Received 17 September 2017
Revised 21 November 2017
Accepted 21 November 2017
Available online 29 December 2017

Keywords:
Super-fine activated carbon
Catalytic ozonation
External surface area
Surface reaction
Hydroxyl radical

ABSTRACT

In this study, super-fine powdered activated carbon (SPAC) has been proposed and investigated as a novel catalyst for the catalytic ozonation of oxalate for the first time. SPAC was prepared from commercial granular activated carbon (GAC) by ball milling. SPAC exhibited high external surface area with a far greater member of meso- and macropores (563% increase in volume). The catalytic performances of activated carbons (ACs) of 8 sizes were compared and the rate constant for pseudo first-order total organic carbon removal increased from 0.012 min^{-1} to 0.568 min^{-1} (47-fold increase) with the decrease in size of AC from 20 to 40 mesh (863 μm) to SPAC (~1.0 μm). Furthermore, the diffusion resistance of SPAC decreased 17-fold compared with GAC. The ratio of oxalate degradation by surface reaction increased by 57%. The rate of transformation of ozone to radicals by SPAC was 330 times that of GAC. The results suggest that a series of changes stimulated by ball milling, including a larger ratio of external surface area, less diffusion resistance, significant surface reaction and potential oxidized surface all contributed to enhancing catalytic ozonation performance. This study demonstrated that SPAC is a simple and effective catalyst for enhancing catalytic ozonation efficacy.

1 Introduction

Industrial wastewater is considered to be among the most severe sources of pollution, owing to the frequent presence of refractory and toxic matter [1]. To remove such refractory organics, advanced oxidation processes (AOPs) are often required [2]. AOPs are a class of efficient technologies in which refractory organics are removed by means of radicals [3]. Among the various AOPs, ozonation is a promising advanced treatment technology due to its non-toxic oxidation products (predominantly water, carbon dioxide, and oxygen) [4]. However, ozone is a selective oxidant and reacts only with certain moieties. Substances

✉ Corresponding authors
E-mail: zhangxiaoyuan@tsinghua.edu.cn (Zhang X Y); xhuang@tsinghua.edu.cn (Huang X)

Special Issue—Advanced Treatment Technology for Industrial Wastewaters (Responsible Editors: Junfeng Niu & Hongbin Cao)

that resist oxidation by ozone alone include carboxyl acids and compounds containing aliphatic chains [5]. Thus, catalytic ozonation has been proposed as an alternative technique. It improves the oxidation performance of ozone by decomposing ozone into radicals. The less-selective radical oxidants allow total mineralization of the refractory matter. Ozone itself decomposes into hydroxyl radicals upon reaction with hydroxides [6,7], but these radicals are generated more efficiently with the help of various catalysts [8]. Such catalysts include homogeneous catalysts and heterogeneous catalysts. Homogeneous catalysts, predominantly transition metal ions [9–12], are not suitable for catalytic ozonation applications because of leaching risks and separation problems [13]. Heterogeneous catalysts, on the other hand, have resulted in enhanced performance. These include carbon-based materials [5,14–17] and metal oxides [8,11,18,19].

Activated carbon (AC) is an effective and low-cost heterogeneous catalyst for ozonation [20,21]. The functional groups and large surface area of AC are the key characteristics for catalytic ozonation. Nitrogen and oxygen functional groups can be strengthened by chemical methods [22], and the increase of oxygen [7,23] and nitrogen groups [24,25] on the surface correlate with enhanced catalytic performance. Nitrogen functional groups increase electron density and thus can be more attractive toward ozone [26]. Oxygen functional groups act as initiator in the chain reaction mechanism [27] and act as adsorption sites in surface reactions [28]. Existing research [24,26,29] shows that surface area correlates positively with catalytic reactivity in the case of AC. Larger surface area increases the number of adsorption sites available for surface reaction [25], enhances the adsorption rate and thus improves the performance of ozonation [28]. Consequently, significant attention is now being given to super-fine powdered activated carbon (SPAC). SPAC is submicron in size and has been proved to be a very effective adsorbent (it can provide 5-fold increase than powdered activated carbon in adsorption capacity) [30–33]. It has large specific external surface area, and contains oxygen functional groups [31]. These characteristics may facilitate the catalytic ozonation process. Even though previous studies have considered the effect of functional groups and surface area, they have not specifically investigated the effect of surface area on catalytic reactivity. A simple method for increasing the surface area, decreasing diffusion resistance and the functional group at the same time has not been developed.

Here we report, for the first time, the application of SPAC as an efficient ozonation catalyst that is easy to prepare. A commonly used catalyst, granular activated carbon (GAC) was chosen as the precursor for the preparation of SPAC and as a benchmark to evaluate the performance of SPAC. The catalytic performance of SPAC in the ozonation of oxalate was investigated and compared with that of GAC at different dosages. To investigate the effect of surface area on the catalytic performance, activated carbon particles with a range of diameters were fabricated by pulverization of GAC and compared. The reaction sites for catalytic ozonation were determined and the impact of external surface area was evaluated using the adsorption rate and O_3 to $\cdot OH$ transformation efficiency (measured by R_{ct} values) [34]. Possible mechanisms of catalytic ozonation by SPAC are discussed in this article.

2 Materials and methods

2.1 Preparation of super-fine powdered activated carbon and activated carbon with different particle sizes

Pristine wood-based GAC (HG 3-1290, Beijing Chemical Works, China), was pretreated in a solution of HCl/HNO_3 (3:1 v/v) under sonication and then rinsed with Milli-Q ultra-pure water (resistivity $\geqslant$ 18 MΩ·cm) to remove impurities [35,36]. AC samples of various particle sizes were obtained by pulverizing pristine AC using a grinder. These were screened using standard sieves with 10, 20, 40, 70, 100, 160, 300, and 800 mesh sizes. AC samples with 20–40 mesh size are referred to as GAC in this article. SPAC samples were fabricated as follows: GAC as precursors were ball milled for 1 h to SPAC using a planetary ball mill (QM-3SP2, Nanjing NanDa Instrument Plant, China) in the slurry state, then filtered through a 0.22 μm membrane (polyvinylidene fluoride, Millipore, USA) and dried in an oven at 104°C overnight.

2.2 Material characterizations

The particle size of all types of activated carbon used in this study was determined by a laser diffraction particle size analyzer under sonication (Beckman LS13320, USA) (Fig. S1). The hydrodynamic diameter of SPAC suspension was characterized by dynamic light scattering (DLS, Beckman DelsaNano C, USA). The zeta potentials of SPAC and 300–800 mesh AC suspensions were analyzed (Beckman DelsaNano C, USA), which were buffered to different pH values using phosphoric acid. The Boehm titration and pH of point zero charge (pH_{pzc}) were determined as previously reported [37,38]. The morphology and size of the samples were characterized by scanning electronic microscopy (SEM, FEI Quanta200, Netherlands). The SEM images and size distributions of these materials can be found in the Supporting Information (SI, Fig. S2). The nitrogen adsorption isotherms were measured using a surface area and porosity analyzer (Micromeritics 2020HD, USA) at 77.4 K. Surface area, external surface area, and pore distribution were determined by the Brunauer-Emmett-Teller (BET) and t-plot methods. X-ray photoelectron spectroscopy (XPS, ESCALAB 250 Xi, USA) was employed to determine the surface chemical composition and functional groups [39].

2.3 Catalytic ozonation tests

Oxalate [40] was selected as the model contaminant, since it is resistant to oxidation by ozone alone ($k < 0.04$ $M^{-1}\cdot s^{-1}$) [41], but vulnerable to radicals ($k_{\cdot OH}$ = ~10^6 $M^{-1}\cdot s^{-1}$) [42]. One-liter of oxalate (Sinopharm Chemical Reagent, China) solution (~0.8 mM, total organic carbon (TOC) = ~20 mg/L) was stirred with a magnetic stirrer at room temperature (20°C). Ozone was generated from pure oxygen using an ozone generator (Tonglin 3S-A3, China) and continuously injected into the oxalate solution through a titanium diffuser. The gaseous ozone concentration was kept at 180–200 mg/L and monitored using a ultraviolet monitor (Limicen UV-300, China). The dissolved ozone was determined by the indigo method [43,44]. SPAC and AC of various size ranges were then separately added at doses of 0.1, 0.5, 1.0, 2.0, 3.0, 4.0 and 5.0 g/L. Samples were taken at intervals using a glass syringe with a 0.22 μm filter and immediately mixed with 1 mL of $Na_2S_2O_3$ solution (0.1 mM) to quench the residual ozone.

R_{ct} describes the ratio of ·OH exposure and O_3 exposure and is used to indicate O_3 into ·OH transformation efficiency as previously mentioned [34]. *p*-chlorobenzoic acid (*p*CBA, Sigma-Alderich) was used as the radical probe. The pH was not buffered and t-butanol aliquots were added (320 μM). An ozone stock solution was prepared in an ice bath by>30 min ozone aeration to reach equilibrium.

2.4 Oxalate adsorption tests

To discern the contribution of oxidation and adsorption, adsorption kinetic tests were carried out. The dose of AC was 2.0 g/L, which was found optimal in catalytic efficacy in this study, and the concentration of oxalate was 100 mg/L, the same as in catalytic ozonation experiments in this study. The method for calculating kinetic constants is described later in the following paragraph. To investigate pore diffusion and external surface adsorption performance, sonication (300 W, 40 kHz) was incorporated into the adsorption process [45]. The pH was not buffered in any of the experiments in this article except for the determination of zeta potential. All chemical reagents used were analytical grade or higher purity grade. All the results obtained in this study are reported as the average of triplicate measurements.

2.5 Analytical methods

TOC was measured using TOC-V (SHIMADZU, Japan). Oxalate concentration was monitored at 210 nm by Agilent HPLC with Atlantis T3 Column (5 μm, 4.6 mm × 150 mm, Waters, USA). The mobile phase was 20 mM NaH_2PO_4 aqueous solution adjusted to a pH of 2.6 with phosphoric acid [46]. *p*CBA concentration was determined by HPLC at 240 nm with Eclipse XBD Column (5 μm, 4.6 mm × 150 mm, Agilent, USA). The mobile phase was 60:40 methanol and pure water solution adjusted to a pH of 2.7 with phosphoric acid. The pH of the suspension was measured using a portable pH meter (Mettler Toledo SevenGo, Switzerland).

2.6 Kinetic analysis

The removal of oxalate was modeled as a pseudo first order reaction for ozonation processes. The removal rate and removal rate constant are given by Eqs. (1) and (2):

$$dC/dt = -k'C, \tag{1}$$

$$\ln(C_t/C_0) = -k't, \tag{2}$$

where C is the TOC or oxalate concentration in the solution, t is the reaction time, C_0 and C_t are the TOC or oxalate concentration when $t = 0$ and $t = t$, respectively, and k' is the pseudo first order reaction rate constant.

The R_{ct} value was calculated by [34]:

$$R_{ct} = \int [\cdot OH]dt / \int [O_3]dt, \tag{3}$$

$$\ln([pCBA]_t/[pCBA]_0) = -k_{\cdot OH/pCBA} R_{ct} \int [O_3]dt, \tag{4}$$

where $k_{\cdot OH/pCBA} = 5 \times 10^9$ $M^{-1}\cdot s^{-1}$ [34].

A pseudo second-order kinetic model was used for the adsorption processes [45]:

$$\frac{t}{q_t} = \frac{1}{k_2 q_e^2} + \frac{1}{q_e}t, \tag{5}$$

where q_e and q_t are the amounts of oxalate adsorbed on AC at equilibrium and at time t respectively, k_2 is the pseudo second-order rate constant.

To further investigate the diffusion resistance, the initial adsorption rate v_0 was also calculated [45]:

$$v_0 = k_2 q_e^2. \tag{6}$$

3 Results and discussion

3.1 Catalytic ozonation performance of SPAC and GAC

All ACs enhanced the degradation of oxalate by ozone when compared to degradation by ozone alone. SPAC (represented by hollow symbols in Fig. 1(a) outperformed GAC (solid symbols) at identical doses during the catalytic ozonation of oxalate. When the concentration of SPAC was 1.0 g/L, more than 90% of TOC was removed within 10 min. When the same concentration of GAC was used over the same time frame, only 3% of TOC was removed. Similar improvement was also obtained at 2.0 g/L. Besides TOC degradation, the pH of the solution and dissolved

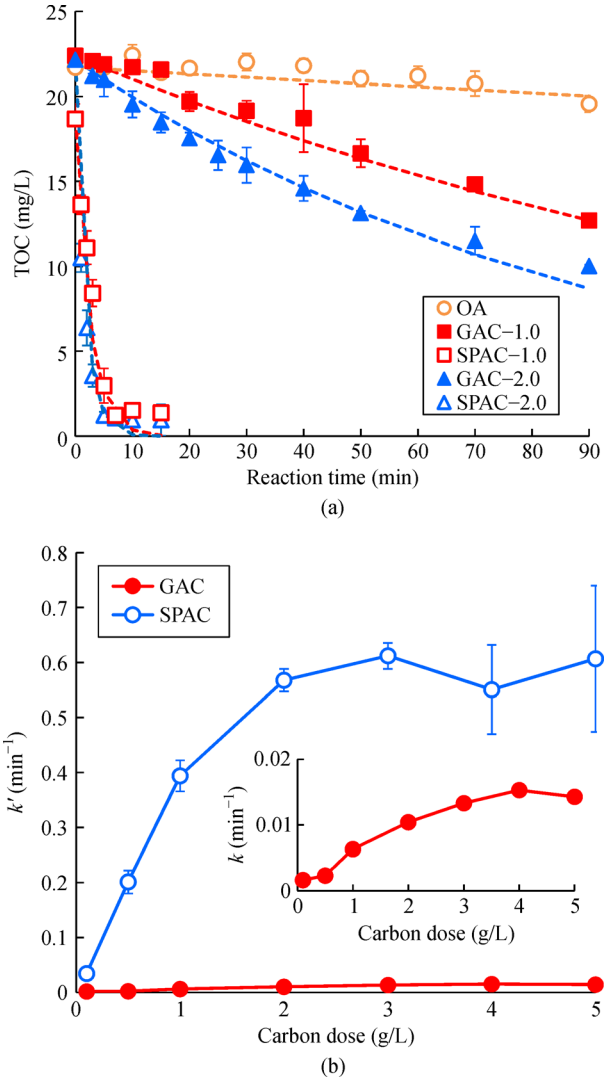

Fig. 1 (a) TOC removal by the catalytic ozonation of oxalate using SPAC and GAC as catalysts over time and (b) pseudo first order rate constants at different SPAC and GAC doses. The dotted lines are kinetic fitting results. The numbers after SPAC and GAC are doses with a unit of g/L. Experimental conditions: oxalate concentration: 100 mg/L, O_3 concentration: 180–200 mg/L, and flow rate: 1.0 L/min. The pH was not buffered

ozone concentration were monitored (Fig. S3). The pH was around 3.1 initially. The final pH of those experiments with SPAC rose to nearly 6.5, whereas pH with GAC was ⩽4.0. This pH increase is believed to have mainly resulted from the degradation of oxalate. Dissolved ozone was also readily decomposed and remained at ~0.2 mg/L for SPAC. It was much higher level for GAC (around 6–7 mg/L). These results showed that SPAC was better at mineralizing oxalate and decomposing ozone GAC.

Regarding TOC degradation, SPAC had much higher catalytic reactivity than GAC from a kinetic perspective (Fig. 1(b)). TOC removal data fits the pseudo first order reaction model (dot lines) well for both SPAC and GAC (R^2>0.95). Kinetic rate constants for the catalytic ozonation of oxalate were compared at different SPAC and GAC dosages (Fig. 1(b)). When the concentration of SPAC was 1.0 g/L, the rate constant was 0.40 min^{-1}, 62 times that of GAC under identical conditions. Furthermore, the rate constants were much higher for SPAC than GAC at all dosages (between 21 and 87 times higher for all dosages 0.1–5.0 g/L). The rate constants for the catalytic ozonation reactions gradually increased with dosage increase for both GAC and SPAC (Fig. 1(b)).

In contrast to GAC, rate constants gradually reached a plateau when the SPAC dosage exceeded 2.0 g/L. This indicates that when the catalyst dose is above 2.0 g/L (i.e. surface area of 1490 m^2 per liter water), it is no longer the limiting factor in the ozonation process. It has been reported that the dose of AC is the factor that determines the number of reaction sites in oxidation [24,47]. A higher dose of carbon is expected to lead to higher catalytic efficacy. However, in this case, higher concentration of SPAC did not lead to a faster degradation. This may be because SPAC deposits differently to GAC when added to water, which will be discussed later. This phenomenon could also be related to surface reactions that are controlled by chemical adsorption and may follow the Langmuir-Hinshelwood or Eley-Rideal mechanisms [48]. The mechanism for chemical adsorption will be the subject of future study.

Catalyst dosage has been identified as a key parameter in determining the efficacy of catalytic ozonation [13]. Thus, to eliminate the kinetic limitations stemming from insufficient SPAC dose and to maximize the catalytic efficacy, 2.0 g/L was chosen as the optimal SPAC dosage and used in subsequent experiments, unless stated otherwise.

3.2 Particle size effect on catalytic ozonation

A series of ACs with a range of diameters were tested as catalysts for ozonation of oxalate, and the catalytic performance significantly increased with the decrease in particle size (Fig. 2(a)). As the carbon size decreased, TOC removal was enhanced. After 20 min, TOC removal was 18% for 10–20 mesh AC (average size: 1351 μm), 42% for 70–100 mesh AC (average size: 248 μm) and 82% for 300–800 mesh AC (average size: 63 μm). When the size decreased to the smallest-SPAC (average size: 1.4 μm), 90% TOC was removed in only 10 min. The dashed lines in Fig. 2(a) show that pseudo first-order kinetics accurately describe (R^2>0.96) TOC removal when ACs with a range of diameters were adopted. The rate constants were 0.008 min^{-1} for 10–20 mesh, 0.012 min^{-1} for 20–40 mesh, 0.026 min^{-1} for 40–70 mesh, 0.027 min^{-1} for 70–100 mesh, 0.077 min^{-1} for 100–160 mesh, 0.323 min^{-1} for 160–300 mesh, 0.343 min^{-1} for 300–800 mesh and 0.568 min^{-1} for the SPAC. The rate constants imply that faster

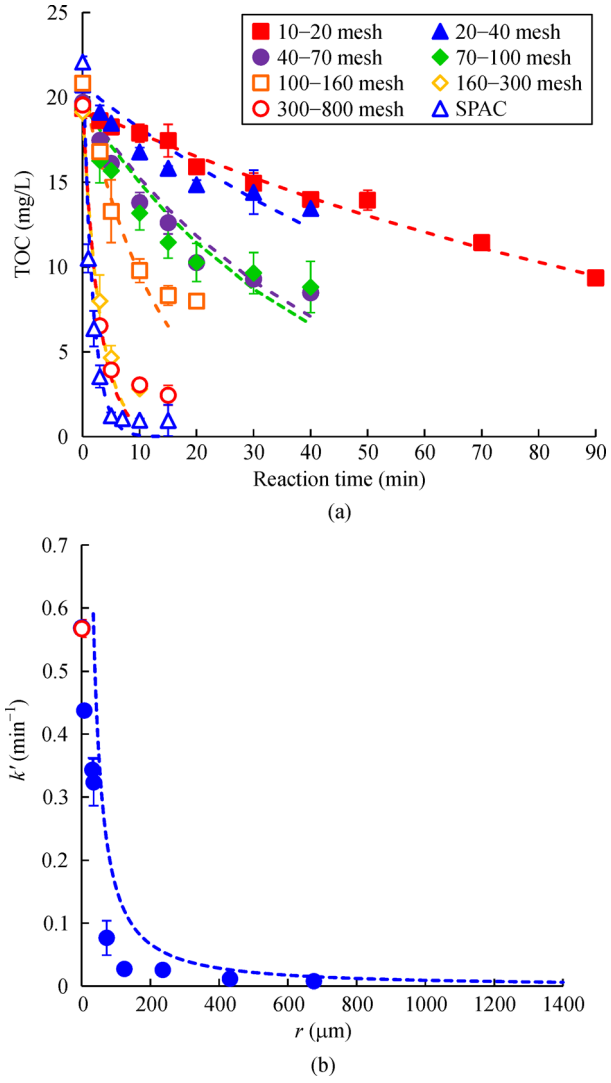

Fig. 2 (a) TOC removal by the catalytic ozonation of oxalate using AC catalysts with various sizes and (b) the relationship between pseudo first-order rate constants and carbon radius. The dotted lines in (a) and (b) are kinetics fitting results and fitting trend. Experimental conditions: oxalate concentration: 100 mg/L, O_3 concentration: 180–200 mg/L, flow rate: 1.0 L/min, carbon dose: 2 g/L. The pH was not buffered

degradation was achieved when carbon size decreased. A clear trend can be found between the rate constants and the average radius of the ACs (Fig. 2(b)). The power of the fitting function was approximately −1. This supports the notion that catalytic ozonation by AC is related to geometric surface area, since the power of the fitting function can be deduced from Eqs. (7)–(9).

$$\text{Surface area of a sphere}: \quad S = 4\pi r^2, \tag{7}$$

$$\text{Volume of a sphere}: \quad V = \frac{4}{3}\pi r^3, \tag{8}$$

$$\text{Geometric surface area}: \quad \frac{S}{m} = \frac{S}{\rho V} = \frac{4\pi r^2}{\frac{4}{3}\rho\pi r^3} = \frac{3}{\rho}\cdot\frac{1}{r}. \tag{9}$$

SPAC was excluded when the above trend was fitted, but it still followed this trend. The power of the fitting function is not strictly −1, thus the reduction in particle size is not the sole factor influencing the improvement in ozonation performance caused by SPAC. Characteristics of SPAC other than surface area have also been investigated and compared with the GACs.

3.3 Other SPAC characteristics favorable to catalytic ozonation

The ability of SPAC to significantly enhance catalytic ozonation performance when compared with GACs may also be related to the following factors: 1) diffusion enhancement; 2) the significance of surface reaction; and 3) favorable surface chemistry and physics.

1) Diffusion enhancement. The primary step of an interface reaction, including heterogeneous catalytic ozonation, is mass diffusion to the reaction sites [49]. Previous discussion neglected oxalate removal by adsorption. It is difficult to assess catalytic activity regardless adsorption by activated carbon [50]. Therefore, oxalate adsorption tests were carried out to determine the amount of removal by adsorption and the diffusion resistance was indicated by adsorption kinetics. In this case, SPAC has a higher ratio of meso- and macropores, which decrease the diffusion resistance of oxalate to AC and enhance the whole reaction rate.

Oxalate adsorption by SPAC and GAC with and without sonication are shown in Fig. 3, accompanied by corresponding kinetic parameters. The dotted and dashed lines in Fig. 3(a) show a good fit (R^2>0.97) with the pseudo second-order model [45] for oxalate adsorption. SPAC and GAC exhibited limited adsorption capacity (30% and 25% oxalate removal over a period of 60 min). SPAC adsorbed oxalate more quickly during the first 10 min. This was confirmed with the pseudo second-order rate constant k_2 (3.2 g/mg/min, Fig. 3(b)) and the initial adsorption rate v_0 (4.6 mg/g/min, Fig. 3(c)) of SPAC, which were 16 and 8 times higher than those of GAC (0.2 g/mg/min and 0.6 mg/g/min). GAC exhibited slower adsorption in the initial stage and did not reach equilibrium within the first 60 min, but had a higher adsorption capacity (18.2 mg/g) than SPAC (13.5 mg/g) at equilibrium (Fig. 3(d)). When sonication was applied for GAC, the adsorption rate accelerated. The initial adsorption rate v_0 almost doubled, from 0.6 to 1.0 mg/g/min, and the amount adsorbed was higher (increased to 22.0 mg/g). However, sonication had a negative effect on the SPAC adsorption process. The initial adsorption rate was slower (decreased to 2.2 mg/g/min) and the adsorption capacity at equilibrium concentration

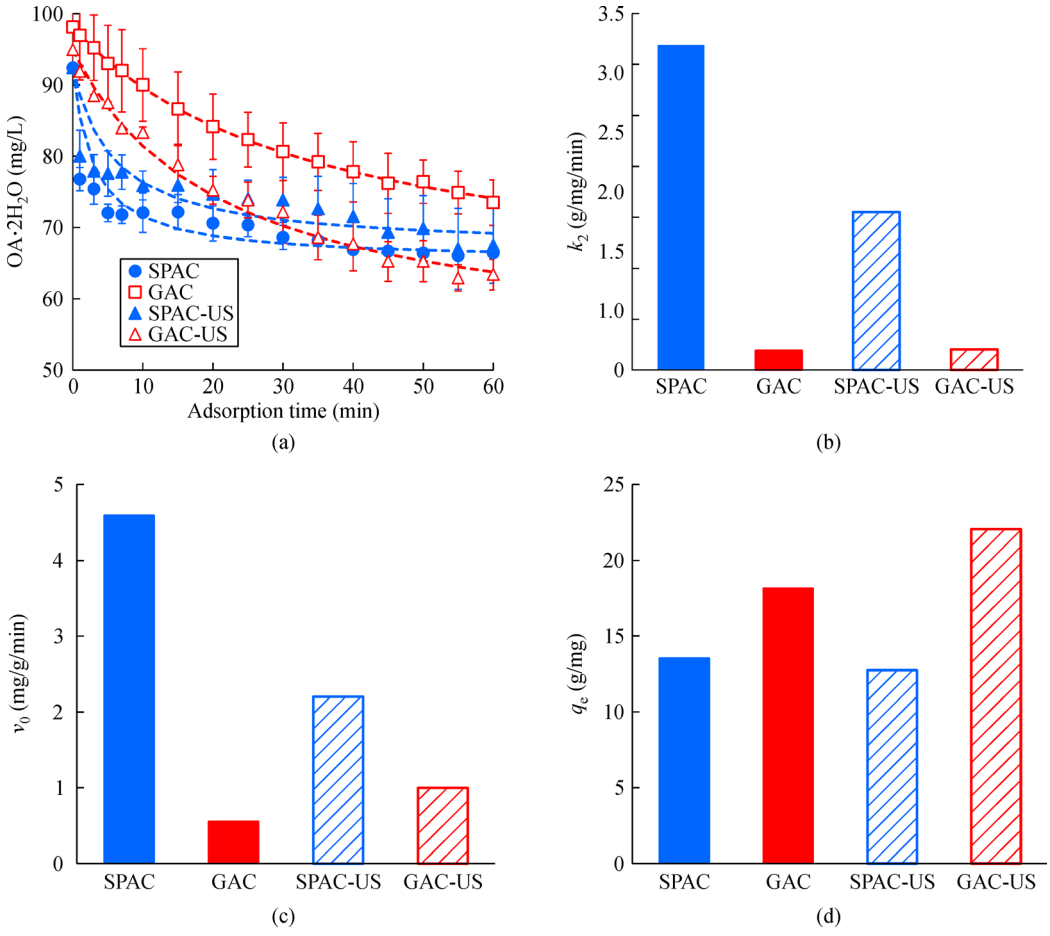

Fig. 3 (a) Adsorption of oxalate by SPAC and GAC with and without sonication; (b) pseudo second-order rate constants; (c) initial adsorption rates; (d) adsorbed oxalate at equilibrium. Experimental conditions: oxalate concentration: 100 mg/L, carbon dose: 2 g/L. The pH was not buffered

was lower (dropped to 12.7 mg/g) compared to results obtained without sonication.

As reported [33], greater external surface area can lead to a faster adsorption. This agreed with our own observation. Sonication is believed to enhance adsorption by enhancing diffusion into micropores for GAC [45], which also agrees with our observation (Fig. 3). However, the applied sonication for SPAC led to a decrease in both the adsorption rate and equilibrium concentration (Fig. 3(a)). Larger external surface area and more meso- and macropores (Table 1) are assumed to be related to fast adsorption by SPAC. Sonication can aid the desorption process and even regenerate the used AC [51,52], so desorption was probably the dominant process for SPAC during sonication.

In general, SPAC achieved a less oxalate diffusion resistance through adsorption kinetics. This may be the result of the higher ratio of meso- and macropores to total pore volume in SPAC. Less diffusion resistance can assist catalytic ozonation.

2) Significance of surface reaction and high ozone-to-radical transformation. Although meso- and macropores were found to be crucial in adsorption and catalytic ozonation, the reaction sites for AC catalyzed ozonation have not been clarified. Oxalate degradation can occur in bulk solution, at the boundary layer, and on particle

Table 1 Surface area characterizations of GAC, 100–160 mesh AC and SPAC

Sample	S_{BET} (m^2/g)	$S^{a,b)}_{micro}$ (m^2/g)	$S^{a)}_{ext}$ (m^2/g)	$V^{a,b)}_{micro}$ (cm^3/g)	$V^{b)}_{meso+macro}$ (cm^3/g)	V_{tot} (cm^3/g)
GAC	456.9±1.9	208.5	248.4	0.0954	0.0316	0.127
100–160 mesh AC	476.2±2.6	220.7	255.4	0.0948	0.1112	0.206
SPAC	745.3±6.1	24.4	720.9	0.0048	0.2102	0.215

Notes: S_{BET} = total specific area by BET method; S_{micro} = specific micropore surface area; S_{ext} = specific external surface area; V_{micro} = specific micropore volume; $V_{meso+macro}$ = specific meso- and macro-pore volume; V_{tot} = specific total pore volume. a) calculated by t-plot method; b) micropores, mesopores and macropores are those pores with diameter < 2 nm, 2–50 nm and>50 nm, respectively

surfaces. Experiments were carried out to determine the reaction sites, including 1) ozonation of oxalate without catalyst, 2) AC catalytic ozonation of oxalate and 3) AC catalytic ozonation of oxalate with t-butanol (Fig. 4). A much faster oxalate removal by catalytic ozonation in 10 min could be observed for SPAC, compared with GAC, both in the conditions with and without t-butanol. It is assumed that radicals in the boundary layer and bulk solution were inhibited by t-butanol. The oxalate removal in the boundary layer can be calculated using 2)–3)–1) by integration of the oxalate concentration to time [53]. It took ~8% for GAC and ~2% for SPAC of total oxalate removal. Due to the weak affinity (Fig. S4) of t-butanol toward AC, the oxalate removal with t-butanol indicated its removal on particle surface. The contribution of surface reaction to total oxalate degradation was 61% for GAC and 96% for SPAC. These results demonstrate that the surface reaction was much stronger for SPAC than GAC and contributed significantly to oxalate degradation when SPAC was used.

Furthermore, the R_{ct} value was calculated to consolidate the ozone-to-radical enhancement in the SPAC catalytic ozonation process. This was done using *p*CBA, which has different affinity toward AC [24,54] when compared with oxalate. The R_{ct} of GAC at 200 mg/L was 1.6×10^{-10}, a 4-fold increase compared with that of ozone alone (4.0×10^{-11}). The R_{ct} of SPAC at the same dosage was 5.3×10^{-8}, a 330-fold increase compared with that of GAC (Fig. 5). This enhancement was not comparable with the only 64% increase in surface area, as the high enhancement was partly caused by the higher affinity of *p*CBA toward SPAC when compared with GAC (Fig. S4). SPAC at 200 mg/L efficiently decomposed ozone into radicals with the similar level of the R_{ct} value of H_2O_2/O_3 (4.3×10^{-8}) [15] (Table S1).

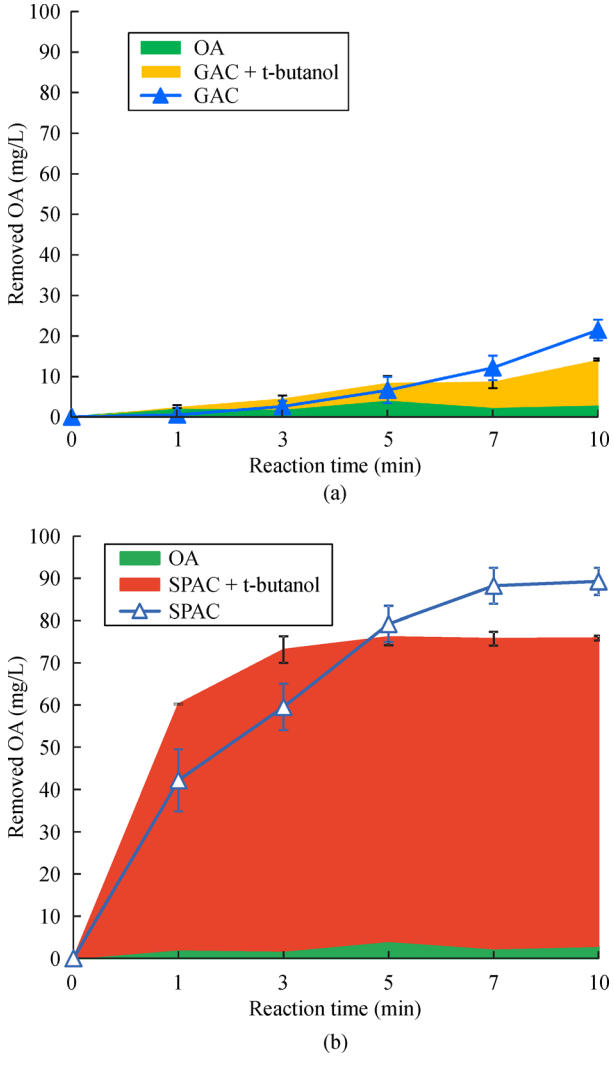

Fig. 4 Oxalate removal by ozone alone (green area), ozone + carbon + t-butanol (yellow, orange area) and ozone + carbon (line) in the case of (a) GAC and (b) SPAC. Experimental conditions: oxalate concentration (OA): 100 mg/L, t-butanol: 1 mM, O_3 concentration: 180–200 mg/L, flow rate: 1.0 L/min, carbon dose: 2 g/L. The pH was not buffered

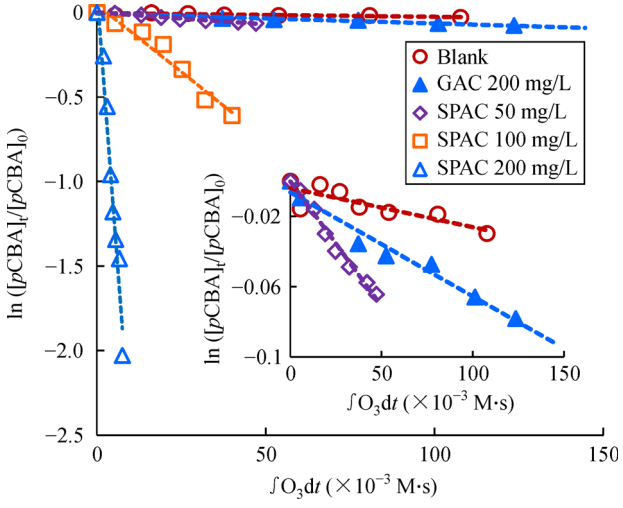

Fig. 5 R_{ct} plots for ozone alone, and ozone with GAC and SPAC at various carbon doses. The slope of the fitting line represents the R_{ct} value. Detailed parameters are shown in Table S1. Experimental conditions: *p*CBA concentration: 2 μM, t-butanol concentration: 320 μM. The pH was not buffered

3) Favorable surface chemistry and physics. Investigations of surface functional groups were conducted by XPS analysis, Boehm titration and pH_{pzc} (pH of point zero charge). XPS analyses indicated that GAC, 100–160 mesh AC and SPAC had similar surface element constitution (Table S2). Boehm titration indicated that these three carbons had a similar number of oxygen-containing groups, although the number was slightly higher for SPAC than for GAC and 100–160 mesh AC (Table S3). After the reaction, the oxygen contents increased and oxygen was mainly present in the form of C = O and O-C = O (Table S2). The pH_{pzc} of SPAC was 5.00±0.02, which was also slightly higher than for GAC (4.02±0.01). This

indicates higher basicity, which helps the decomposition of ozone into radicals [55,56] (Fig. S5). As mentioned in a previous study [31], rapid oxidation occurs at the external sites of AC during the ball milling process. The change in pH_{pzc} is likely to be related to this phenomenon and thus would potentially improve the catalytic reactivity of AC.

The BET surface area of SPAC was 745.3 m^2/g, 63% higher than that of GAC (456.9 m^2/g) (Table 1). The proportion of total SPAC surface area that was external surface area was 96.7%, compared to 54.5% for GAC. After ball milling, the meso- and macro- pore volume of SPAC was 0.21 cm^3/g, ~2 times that of 100–160 mesh AC and 7 times that of GAC (Table 1).

The zeta potential changes for SPAC and 300–800 mesh AC are graphed against pH in Fig. S6. SPAC and 300–800 mesh AC were negatively charged when pH>3.2. The zeta potential of both increased to above zero when pH decreased. SPAC suspension is unstable when the absolute value of zeta potential falls below 5 mV, which corresponds to a pH range of 3.12–3.39. Coincidently, the initial pH of the oxalate solution applied in this study was ~3.12. Therefore, a strong agglomeration [57] was expected at the beginning of the catalytic ozonation of oxalate.

To further investigate the agglomeration in SPAC suspension, hydrodynamic diameters at different SPAC doses were determined, as shown in Fig. S6. All the average hydrodynamic diameters of SPAC were higher than solid state at 2.0–5.0 g/L. They became larger as the dose increased. A 2-fold and a 6-fold increase were observed at 2.0 and 5.0 g/L, respectively, compared with that in solid state. This phenomenon can be related to the plateau observed in Fig. 1(b). When the concentration of SPAC increases, its suspension has more tendency to agglomerate. This is also favored by the pH condition provided by oxalate solution. Therefore, this phenomenon might explain why rate constants no longer increased when the dosage was above 2.0 g/L.

In summary, besides the larger surface area and external surface area provided by SPAC, the change in pore structures, the potential oxidized external surface would also result in less diffusion resistance, significant surface reaction and overall higher catalytic reactivity compared with GAC. Among these properties, larger external surface area (190% increase in area) was the most important and fundamental factor and was accompanied by larger meso- and macropore structure (563% increase in volume). These two factors led to less diffusion resistance (1560% increase in k_2) and more significant surface reaction (oxalate removal by surface reaction increased from 61% to 96%). Therefore, the much higher reactivity of SPAC (47-fold increase in oxalate degradation kinetics) was not solely due to limited surface area change (63% increase) but instead due to the combined effect of a series of AC modification by ball milling.

3.4 Discussion of possible mechanisms

SPAC catalytic ozonation greatly improved oxalate degradation compared with GAC. This improvement is related to a series of favorable changes brought about by ball milling, rather than to one sole factor.

In the case of heterogeneous catalytic ozonation, homogeneous chain reaction and heterogeneous surface reaction are believed to occur simultaneously [49]. AC can act as the initiator of the chain reaction to accelerate the decomposition of ozone into radicals in bulk solution [27]. It is also possible that surface reactions will occur [5,47].

In this study, given the pH condition and the determination of reaction sites, homogeneous reactions would be minor in the SPAC catalyzed ozonation process. As previously discussed, low pH and t-butanol inhibits radicals in the bulk solution and boundary layer, but oxalate removal by SPAC catalyzed ozonation was not influenced by t-butanol. Thus it can be deduced that surface reaction was significant. The surface reaction may have occurred according to the Langmuir-Hinshelwood mechanism, as has been reported in a previous study [5]. The following reactions may describe the pathway of the SPAC catalyzed ozonation process [5]:

Reaction with ozone to form oxygen-containing radicals:

$$AC + O_3 \rightarrow AC - O\cdot \quad (10)$$

Adsorption of organics (R):

$$AC + R \rightarrow AC - R \quad (11)$$

Reaction between adsorbed species:

$$AC - O\cdot + AC - R \rightarrow \text{Products} \quad (12)$$

There is also a possibility that the surface reaction mechanism followed the Eley-Rideal mechanism. This mechanism is similar to the above reactions (Eqs. (10)–(11)), but organics (R) would be directly oxidized by AC-O· as Eq. (13):

$$AC - O\cdot + R \rightarrow \text{Products} \quad (13)$$

Regardless of the mechanism that best describes the process, the surface reaction was certainly dominant, especially in the case of SPAC. The larger external surface area of SPAC provided more sites for adsorption of oxalate. Additionally, not only does the number of reaction sites increase, the kinetic accessibility of these sites is also enhanced. SPAC provided larger external surface area with more meso- and macropores, resulting in a less diffusion resistance than GAC. SPAC had much greater external surface area due to a greater number of meso- and macropores. This reduced diffusion resistance and resulted in a much faster degradation of oxalate. The determination of the radical exposure (R_{ct}) value supports this conclusion.

SPAC was not only more effective when applied to oxalate, it also effectively degraded *p*CBA, which has a different affinity toward AC (Fig. S4). Yet due to a different suspension character, super-fine powders attract each other and agglomerate when pH is near pH_{IEP} (pH value at isoelectric point; i.e., the pH value when zeta potential was zero). The agglomeration jeopardizes the efficacy of catalytic ozonation by causing a higher hydrodynamic diameter and blockage of active surface sites. This phenomenon was observed at high doses of SPAC. And further investigation on whether the surface reactions exaggerated by SPAC followed Langmuir-Hinshelwood or Eley-Rideal mechanism [48] will be studied in the future. Besides, ceramic membrane is considered to be capable to separate SPAC from water and recycle and can be investigated.

4 Conclusions

SPAC performed significantly better than GAC during catalytic ozonation of oxalate and the catalytic efficacy was influenced by carbon dosage and diameter. Rate constant was found to be closely related with the geometric surface area of the carbon particle. There are multiple changes in the material characteristics of SPAC benefiting the efficacy of catalysis. Besides more reaction sites, large external surface reduced the diffusion resistance, leading to a faster adsorption. Meanwhile, SPAC has more oxidized surface and basicity, which can further enhance the catalysis performance. It was found that, in the case of SPAC, the surface of the carbon particle is responsible for the catalytic ozonation, where almost all oxalate was degraded. SPAC had much higher transformation rate from ozone to hydroxyl radicals (investigated as R_{ct} value). Simple ball milling can bring a series of material modification of activated carbon. These results provide a proof-of-concept for SPAC as a better-performing and cost-effective catalyst of ozonation, and highlight that external surface area is a critical factor when AC is used in catalytic ozonation processes.

Acknowledgements This research was supported by the National Key Research and Development Program-China (No. 2016YFB0600502) and funding from the State Key Joint Laboratory of Environment Simulation and Pollution Control (No. 15Y02ESPCT).

Electronic Supplementary Material Supplementary material is available in the online version of this article at http://dx.doi.org/10.1007/s11783-018-1022-2 and is accessible for authorized users.

References

1. Khamparia S, Jaspal D K. Adsorption in combination with ozonation for the treatment of textile waste water: A critical review. Frontiers of Environmental Science & Engineering, 2017, 11(1): 8
2. Oller I, Malato S, Sánchez-Pérez J A. Combination of advanced oxidation processes and biological treatments for wastewater decontamination—A review. Science of the Total Environment, 2011, 409(20): 4141–4166
3. Matilainen A, Sillanpää M. Removal of natural organic matter from drinking water by advanced oxidation processes. Chemosphere, 2010, 80(4): 351–365
4. Bard A J, Faulkner L R. Electrochemical Methods: Fundamentals and applications. 2nd ed.New York: John Wiley and Sons Inc., 2001
5. Faria P C C, Órfão J J M, Pereira M F R. Activated carbon catalytic ozonation of oxamic and oxalic acids. Applied Catalysis B: Environmental, 2008, 79(3): 237–243
6. Staehelin J, Hoigne J. Decomposition of ozone in water in the presence of organic solutes acting as promoters and inhibitors of radical chain reactions. Environmental Science & Technology, 1985, 19(12): 1206–1213
7. Alvárez P, García-Araya J, Beltrán F, Giráldez I, Jaramillo J, Gμmez-Serrano V. The influence of various factors on aqueous ozone decomposition by granular activated carbons and the development of a mechanistic approach. Carbon, 2006, 44(14): 3102–3112
8. Legube B, Leitner N K V. Catalytic ozonation: A promising advanced oxidation technology for water treatment. Catalysis Today, 1999, 53(1): 61–72
9. Ma J, Graham N J D. Degradation of atrazine by manganese-catalysed ozonation: Influence of humic substances. Water Research, 1999, 33(3): 785–793
10. Pines D S, Reckhow D A. Effect of dissolved cobalt(II) on the ozonation of oxalic acid. Environmental Science & Technology, 2002, 36(19): 4046–4051
11. Beltrán F J, Rivas F J, Montero-de-Espinosa R. Iron type catalysts for the ozonation of oxalic acid in water. Water Research, 2005, 39 (15): 3553–3564
12. Andreozzi R, Caprio V, Insola A, Marotta R, Tufano V. The ozonation of pyruvic acid in aqueous solutions catalyzed by suspended and dissolved manganese. Water Research, 1998, 32 (5): 1492–1496
13. Nawrocki J, Kasprzyk-Hordern B. The efficiency and mechanisms of catalytic ozonation. Applied Catalysis B: Environmental, 2010, 99(1–2): 27–42
14. Fan X, Restivo J, Órfão J J M, Pereira M F R, Lapkin A A. The role of multiwalled carbon nanotubes (MWCNTs) in the catalytic ozonation of atrazine. Chemical Engineering Journal, 2014, 241: 66–76
15. Oulton R, Haase J P, Kaalberg S, Redmond C T, Nalbandian M J, Cwiertny D M. Hydroxyl radical formation during ozonation of multiwalled carbon nanotubes: performance optimization and demonstration of a reactive CNT filter. Environmental Science & Technology, 2015, 49(6): 3687–3697
16. Rocha R P, Gonçalves A G, Pastrana-Martínez L M, Bordoni B C, Soares O S G P, Órfão J J M, Faria J L, Figueiredo J L, Silva A M T, Pereira M F R. Nitrogen-doped graphene-based materials for advanced oxidation processes. Catalysis Today, 2015, 249: 192–198
17. Restivo J, Garcia-Bordejé E, Órfão J J M, Pereira M F R. Carbon nanofibers doped with nitrogen for the continuous catalytic

ozonation of organic pollutants. Chemical Engineering Journal, 2016, 293: 102–111

18. Zhang T, Li C, Ma J, Tian H, Qiang Z. Surface hydroxyl groups of synthetic α-FeOOH in promoting ·OH generation from aqueous ozone: Property and activity relationship. Applied Catalysis B: Environmental, 2008, 82(1–2): 131–137
19. Zhang T, Li W, Croué J P. Catalytic ozonation of oxalate with a cerium supported palladium oxide: An efficient degradation not relying on hydroxyl radical oxidation. Environmental Science & Technology, 2011, 45(21): 9339–9346
20. Marsh H. Introduction to Carbon Technologies. Alicante: University of Alicante, 1997
21. Figueiredo J L, Pereira M F R. The role of surface chemistry in catalysis with carbons. Catalysis Today, 2010, 150(1–2): 2–7
22. Figueiredo J L, Pereira M F R, Freitas M M A, Orfao J J M. Modification of the surface chemistry of activated carbons. Carbon, 1999, 37(9): 1379–1389
23. Krzyżyńska B, Malaika A, Rechnia P, Kozłowski M. Study on catalytic centres of activated carbons modified in oxidising or reducing conditions. Journal of Molecular Catalysis A Chemical, 2014, 395: 523–533
24. Sánchez-Polo M, von Gunten U, Rivera-Utrilla J. Efficiency of activated carbon to transform ozone into *OH radicals: influence of operational parameters. Water Research, 2005, 39(14): 3189–3198
25. Xing L, Xie Y, Cao H, Minakata D, Zhang Y, Crittenden J C. Activated carbon-enhanced ozonation of oxalate attributed to HO● oxidation in bulk solution and surface oxidation: Effects of the type and number of basic sites. Chemical Engineering Journal, 2014, 245: 71–79
26. Cao H, Xing L, Wu G, Xie Y, Shi S, Zhang Y, Minakata D, Crittenden J C. Promoting effect of nitration modification on activated carbon in the catalytic ozonation of oxalic acid. Applied Catalysis B: Environmental, 2014, 146: 169–176
27. Jans U, Hoigne J. Activated carbon and carbon black catalyzed transformation of aqueous ozone into OH-radicals. Ozone Science and Engineering, 1998, 20(1): 67–90
28. Álvarez P M, Masa F J, Jaramillo J, Beltran F J, Gomezserrano V. Kinetics of ozone decomposition by granular activated carbon. Industrial & Engineering Chemistry Research, 2008, 47(8): 2545–2553
29. Qiao N, Zhang X, He C, Li Y, Zhang Z, Cheng J, Hao Z. Enhanced performances in catalytic oxidation of o-xylene over hierarchical macro-/mesoporous silica-supported palladium catalysts. Frontiers of Environmental Science & Engineering, 2016, 10(3): 458–466 doi:10.1007/s11783-015-0802-1
30. Bonvin F, Jost L, Randin L, Bonvin E, Kohn T. Super-fine powdered activated carbon (SPAC) for efficient removal of micropollutants from wastewater treatment plant effluent. Water Research, 2016, 90: 90–99
31. Partlan E, Davis K, Ren Y, Apul O G, Mefford O T, Karanfil T, Ladner D A. Effect of bead milling on chemical and physical characteristics of activated carbons pulverized to superfine sizes. Water Research, 2016, 89: 161–170
32. Matsui Y, Ando N, Yoshida T, Kurotobi R, Matsushita T, Ohno K. Modeling high adsorption capacity and kinetics of organic macromolecules on super-powdered activated carbon. Water Research, 2011, 45(4): 1720–1728
33. Ando N, Matsui Y, Kurotobi R, Nakano Y, Matsushita T, Ohno K. Comparison of natural organic matter adsorption capacities of super-powdered activated carbon and powdered activated carbon. Water Research, 2010, 44(14): 4127–4136
34. Elovitz M S, von Gunten U. Hydroxyl radical/ozone ratios during ozonation processes. I. The R_{CT} concept. Ozone Science and Engineering, 1999, 21(3): 239–260
35. Rivera-Utrilla J, Sánchez-Polo M. Ozonation of 1,3,6-naphthalene-trisulphonic acid catalysed by activated carbon in aqueous phase. Applied Catalysis B: Environmental, 2002, 39(4): 319–329
36. Nawrocki J, Fijołek L. Catalytic ozonation—Effect of carbon contaminants on the process of ozone decomposition. Applied Catalysis B: Environmental, 2013, 142–143: 307–314
37. Boehm H P. Chemical Identification of Surface Groups. Advances in Catalysis, 1966, 16: 179–274
38. Dastgheib S A, Karanfil T, Cheng W. Tailoring activated carbons for enhanced removal of natural organic matter from natural waters. Carbon, 2004, 42(3): 547–557
39. Valdés H, Sánchez-Polo M, Rivera-Utrilla J, Zaror C A. Effect of ozone treatment on surface properties of activated carbon. Langmuir, 2002, 18(6): 2111–2116
40. Vecitis C D, Lesko T, Colussi A J, Hoffmann M R. Sonolytic decomposition of aqueous bioxalate in the presence of ozone. The Journal of Physical Chemistry A, 2010, 114(14): 4968–4980
41. Hoigné J, Bader H. Rate constants of reactions of ozone with organic and inorganic compounds in water—II: Dissociating organic compounds. Water Research, 1983, 17(2): 185–194
42. Sehested K, Getoff N, Schwoerer F, Markovic V M, Nielsen S O. Pulse radiolysis of oxalic acid and oxalates. Journal of Physical Chemistry, 1971, 75(6): 749–755
43. Bader H, Hoigne J. Determination of ozone in water by the indigo method. Water Research, 1981, 15(4): 449–456
44. American Water Works Association (AWWA) A P H A A. Standard Methods for the Examination of Water and Wastewater. 22nd Ed. Washington, DC: Water Environment Federation, 2012
45. Zhao D, Cheng J, Vecitis C D, Hoffmann M R. Sorption of perfluorochemicals to granular activated carbon in the presence of ultrasound. The Journal of Physical Chemistry A, 2011, 115(11): 2250–2257
46. Wang H, Yuan S, Zhan J, Wang Y, Yu G, Deng S, Huang J, Wang B. Mechanisms of enhanced total organic carbon elimination from oxalic acid solutions by electro-peroxone process. Water Research, 2015, 80: 20–29
47. Xing L, Xie Y, Minakata D, Cao H, Xiao J, Zhang Y, Crittenden J C. Activated carbon enhanced ozonation of oxalate attributed to HO oxidation in bulk solution and surface oxidation: Effect of activated carbon dosage and pH. Journal of Environmental Sciences (China), 2014, 26(10): 2095–2105
48. Fogler H S. Elements of Chemical Reaction Engineering, 3rd Ed. Upper Saddle River, NJ: Prentice Hall PTR, 1999
49. Beltrán F J, Rivas J, Álvarez P, Montero-de-Espinosa R M. Kinetics of heterogeneous catalytic ozone decomposition in water in an activated carbon. Ozone Science and Engineering, 2002, 24(4): 227–237
50. Wang J, Cheng J, Wang C, Yang S, Zhu W. Catalytic ozonation of

dimethyl phthalate with RuO_2/Al_2O_3 catalysts prepared by microwave irradiation. Catalysis Communications, 2013, 41: 1–5

51. Breitbach M, Bathen D. Influence of ultrasound on adsorption processes. Ultrasonics Sonochemistry, 2001, 8(3): 277–283
52. Liu C, Sun Y, Wang D, Sun Z, Chen M, Zhou Z, Chen W. Performance and mechanism of low-frequency ultrasound to regenerate the biological activated carbon. Ultrasonics Sonochemistry, 2017, 34: 142–153
53. Park J S, Choi H, Cho J. Kinetic decomposition of ozone and parachlorobenzoic acid (pCBA) during catalytic ozonation. Water Research, 2004, 38(9): 2285–2292
54. von Gunten U. Ozonation of drinking water: Part I. Oxidation kinetics and product formation. Water Research, 2003, 37(7): 1443–1467
55. Alvárez P M, García-Araya J F, Beltrán F J, Giráldez I, Jaramillo J, Gμmez-Serrano V. The influence of various factors on aqueous ozone decomposition by granular activated carbons and the development of a mechanistic approach. Carbon, 2006, 44(14): 3102–3112
56. Faria P C C, Órfão J J M, Pereira M F R. Ozone decomposition in water catalyzed by activated carbon: Influence of chemical and textural properties. Industrial & Engineering Chemistry Research, 2006, 45(8): 2715–2721
57. Chen C, Huang W. Aggregation kinetics of nanosized activated carbons in aquatic environments. Chemical Engineering Journal, 2017, 313: 882–889